13.4 A HIGH RESOLUTION NUMERICAL SIMULATION OF THE LANDFALL OF HURRICANE OPAL (1995)

Glen Romine* and Robert Wilhelmson
University of Illinois at Urbana-Champaign, Urbana, Illinois

1. INTRODUCTION

Landfalling hurricanes are frequently accompanied by severe weather, which may extend well outward from the cyclone center. High winds, destructive storm surge and torrential rainfall often occur near the hurricane core. The public generally recognizes these threats near the center of the cyclone, but is less aware of the fact that severe weather can occur well away. In fact, the actual threat of localized severe weather is often maximized at a distance of 200-400 km from the eye in outer hurricane rainbands, where shear and buoyancy are favorable for the generation of tornado producing storms (McCaul 1991).

Recent high-resolution simulations within the modeling community are providing novel insight into the role of convective scale processes in hurricane organization and evolution. Using models at cloud-scale horizontal resolution, it is now also possible to resolve individual convective elements within their parent hurricane environment. This study examines a high-resolution (1.1 km) simulation of Hurricane Opal (1995) carried out using the MM5. The primary emphasis for this study is investigating convective scale processes associated with outer rainbands and their relationship to the larger scale circulation and organization.

2. METHODOLOGY

Numerical simulations of Hurricane Opal were conducted using the MM5V3.4 on the O2K supercomputer at the National Center for Supercomputing Applications. The model atmospheric conditions were initialized using the ECMWF analyses from 02 – 07 October, 1995, obtained from the NCAR DSS archive. The sea surface temperatures were extracted from the National Meteorological Center (NMC) analyses for the same time period.

The initial conditions were interpolated to the coarse outer MM5 grid of 90 km resolution from the surface to 70 mb. Two-way nested grids were used to achieve the level of resolution required to reasonably represent the diminutive tropical cyclone convective elements, from 30, 10, 3.333 to 1.111 km. The nested grids were only initiated once the disturbance was well enclosed within the nest boundaries to reduce errors related to boundary interactions. Additionally, 35 vertical layers were employed, from the surface to 70 mb with significantly increased resolution in the lowest few kilometers.

Betts-Miller cumulus parameterization was chosen for the outer three grids. Reisner mixed-phase explicit microphysics was used on all grids, exclusively for the inner two grids. The Blackadar boundary layer scheme was employed, not so much for its performance on this case but for the capability to nudge with this physics option, as was deemed necessary to correct early track errors. Nudging of the wind and temperature fields was exercised for the first 24 hours of simulation. The CCM2 radiation scheme, five layer soil model, and shallow convection scheme round out some of the key physics options selected for this simulation.

3. RESULTS

Investigation of the MM5 simulation results reveals rainband structures quite similar to those observed, including convective elements embedded in the outer hurricane rainbands. A sample radar image from a few hours prior to the landfall of Hurricane Opal is given in Fig. 1. Note the outer rainband with numerous embedded convective elements. These elements exhibit structure and behavior

* *Corresponding author address:* Glen Romine, Dept. of Atmospheric Sciences, University of Illinois Urbana-Champaign, 105 S. Gregory St., Urbana, IL 61801; email:romine@atmos.uiuc.edu
Additional information is available on the web at: http://pampa.ncsa.uiuc.edu/~romine/opal.html

analogous to supercells, with persistent, rotating updrafts.

For comparison, the simulated hydrometeor field is given in Fig. 2. Significant differences include the spatial coverage of stratiform precipitation near the outer rainband, and the considerable separation of the outer rainbands from the hurricane core. However, the asymmetric rainfall distribution is well captured. Convective elements within the bands also show greater spatial separation than was observed. Fig. 3 demonstrates a cross-section through a convective element from the simulation, showing a strong low-level updraft and the attendant hydrometeor field. The relative vertical vorticity in this updraft exceeds 0.01 s^{-1} in magnitude. Cell dimensions were similar to those observed and the position and orientation of the outer rainband was reasonably well represented.

The simulated convective environment in which the cells formed was conditionally unstable, highlighted by bands of dry air entrained into the otherwise saturated and nearly moist-adiabatic environment. The CAPE in the environment of the outer rainband was modest (800-1500 JKg^{-1}), yet showed considerable variability on the smallest scales, varying by as much as an order of magnitude over ten kilometers. Most outer rainband cells developed over the warmer Gulf of Mexico waters in a favorable convective environment and then progressed onshore, maintaining strength as they progressed inland across the Florida Panhandle coastline despite an increasingly hostile environment. Cells formed in broken convective lines collocated with bands of mid-tropospheric dry air. The presence of the dry air may play a role in both the evolution of individual convective elements and the linear rainband organization.

Simulated convective cells generally lacked organized downdrafts, and updrafts rarely exceeded 12 ms^{-1}. Linearly organized individual cells in the outer rainband appear to be associated with elongated bands of both horizontal (enhanced local vertical shear) and vertical vorticity. Large values of shear were generally confined to the lowest 5 km, with 0-3 km helicity values over 400 m^2s^{-2} and BRNSHR of 50 m^2s^{-2}. Using the criteria of Stensrud et al. (1997), tornadic supercells are likely. Application of this method is demonstrated for a time near landfall in Fig. 4. The regions without shading meet the entire criterion, whereas shaded regions violate one or more criteria. The criteria thresholds are BRNSHR greater than 40 m^2s^{-2} or less than 120 m^2s^{-2}, CAPE greater than 500 JKg^{-1}, and SREH greater than 150 m^2s^{-2}. Vertical velocity contours, shown in heavy bold overlain on Fig. 4, indicate the locations of convective updrafts. Thus, convection often was present along the edge of the region of favorable conditions.

Standard shear indices, used primarily in Great Plains convection, considerably exaggerated the probable risk of significant tornadoes. Despite the relative weakness in instability, combined shear and instability indices such as EHI, BRN and VGP, also were exceedingly elevated. Instability was vertically elongated and hence vertical buoyancy accelerations were quite small. This may have limited the effectiveness of the updrafts to capitalize on the large environmental shear. Simulated convection was generally rather shallow, with even the strongest cells confined below 10 km, with peak updraft velocities near 700 mb. This shallow convective nature is consistent with observations.

Convective cells favorably modify storm-relative environmental buoyancy and shear from those of the broader mesoscale environment, as was also found in cloud-scale simulations by Brooks *et al.* (1994). This environment-modifying behavior aided cells progressing into regions less convectively favorable for supporting supercells, while on the storm scale conditions remained robust. The surface friction gradient across the Florida coastline is apparent in the magnitudes of low-level shear indices, with higher low-level shear values inland. Additionally, heat and moisture fluxes drop off markedly across the shoreline. Hence, storm-scale modification of the local convective environment in part compensates for the lower instability north of the shoreline, and is aided by increased storm-relative helicity across the boundary. Storms maintained intensity for a while after crossing the shoreline boundary. The updraft strength is likely maintained by increasing dynamical forcing (McCaul and Weisman 1996, 2001) despite progressively decreasing buoyancy. Cells organized in bands generally progressed further inland before weakening than did isolated convective cells.

Another interesting feature noted with cells crossing the coastline is that some cells

demonstrated a marked increase in cyclonic vertical vorticity at low levels in the updraft. Frictional coupling could aid in backing the low-level winds and hence increase the magnitude of streamwise vertical vorticity ingested by the updraft. This may in turn aid the dynamic forcing of the vertical pressure gradient and hence provide a positive feedback mechanism.

A noted minor deficiency in the Opal simulation is the azimuthal orientation of the greatest convective threat and the radial distance from the parent cyclone relative to the observed event. The simulation highlighted the greatest threat region to occur farther from the parent cyclone and later relative to the time of landfall. The observed event featured most of the tornadic threat occurring in the hours just prior to landfall, whereas the simulation convection meeting the tornadic supercell criteria remained mostly offshore until after the system made landfall, 150 km further East. The simulation had much greater spatial separation between the primary and outer rainbands than was observed.

This study suggests that the convective environment as well as the convection itself can be reasonably represented in a numerical simulation of sufficient resolution using the MM5. Standard indices for the evaluation of severe convective potential appear misrepresentative of the convective character which develops in that environment. This offset is primarily driven by the considerable cyclonic shear present in the right front quadrant of the hurricane. Instability profiles within the simulation agree with both observations from Hurricane Opal and with the composite close-proximity thermodynamic profiles of McCaul (1991). Convection forms in environments favorable for tornadic supercell convection by the criteria of Strensrud *et al.* (1997). Despite progressing into adjacent regions which appear unfavorable, the convection still maintains intensity for a modest period of time, and occasionally shows increased cyclonic vertical vorticity. Lastly, even with high resolution, prediction of the region of greatest threat for tornadic convection associated with a landfalling hurricane is not easily captured.

Future efforts include determining a more appropriate descriptor of the convective environment and gaining a better understanding of the convective behavior. Results from these deeper investigations will be presented at the conference, along with some visualizations that have evolved out of this research effort.

4. REFERENCES

Brooks, H. E., C. A. Doswell III, Jeremy Cooper, 1994: On the Environments of Tornadic and Nontornadic Mesocyclones. *Weather and Forecasting*: **9**, 606–618.

McCaul Jr., E. W., 1991: Buoyancy and Shear Characteristics of Hurricane-Tornado Environments. *Monthly Weather Review*: **119**, No. 8, 1954–1978.

McCaul Jr, E. W., Weisman M. L., 1996: Simulations of Shallow Supercell Storms in Landfalling Hurricane Environments. *Monthly Weather Review*, **124**, 408–429.

_____, _____, 2001: The Sensitivity of Simulated Supercell Structure and Intensity to Variations in the Shapes of Environmental Buoyancy and Shear Profiles. *Monthly Weather Review*, **129**, 664–687.

Stensrud, D. J., J. V. Cortinas Jr., H. E. Brooks, 1997: Discriminating between tornadic and nontornadic thunderstorms using mesoscale model output. *Weather and Forecasting*, **12**, 613–632.

5. ACKNOWLEGEMENTS

The authors gratefully acknowledge the support of NSF 99-86672, the use of NCSA computer resources, and the advising of Mohan Ramamurthy and Brian Jewett.

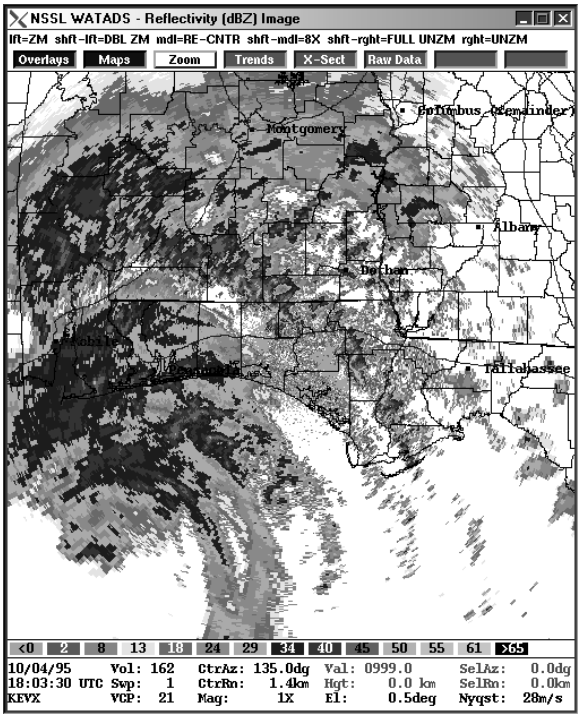

Fig. 1. Base reflectivity from the Elgin AFB WSR-88D showing the outer rainbands associated with Hurricane Opal four hours prior to landfall. The hurricane eye is in the lower-left corner of the image.

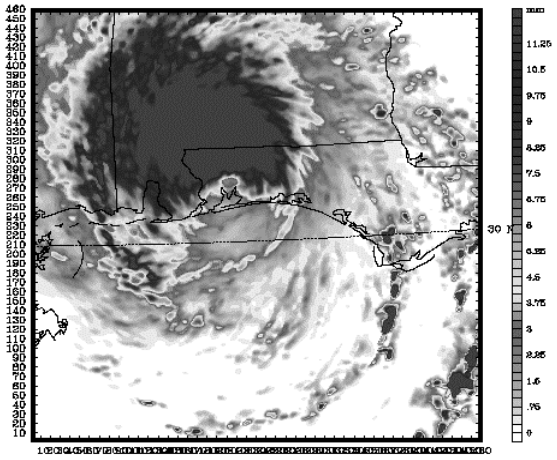

Fig. 2. Hydrometeor distribution for the Hurricane Opal simulation just after landfall. Two outer rainbands are noted along the eastern periphery of the hurricane with a large stratiform region north of the eye.

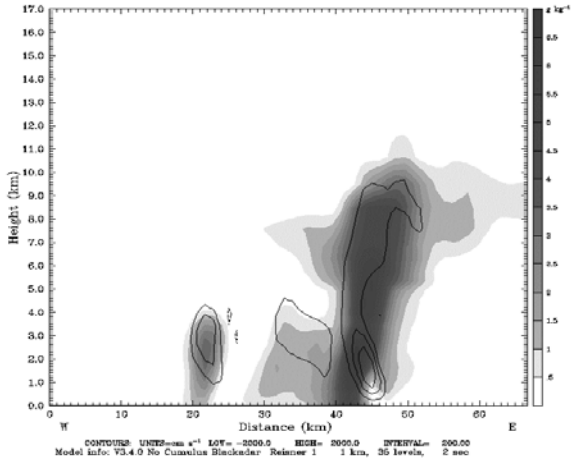

Fig. 3. E-W cross-section through a simulated tropical cyclone convective element in an outer hurricane rainband. The shading indicates hydrometeor mixing ratio concentration, overlain with contours of vertical velocity in 2 ms^{-1} intervals.

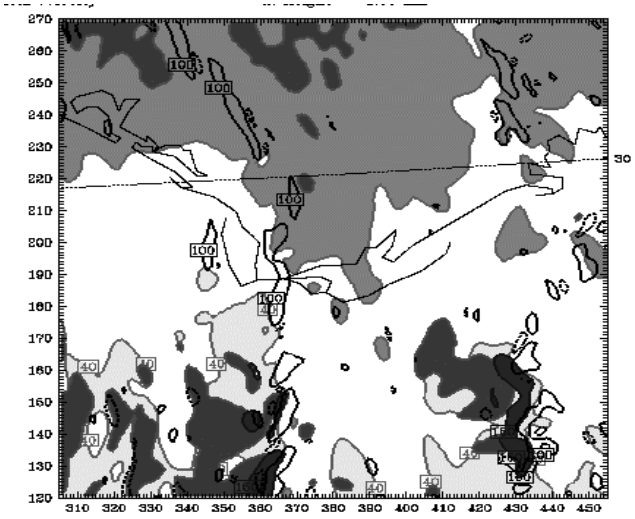

Fig. 4. Composite of Bulk Richardson Number Shear, CAPE, and Storm-Relative Helicity for a quadrant of the 1.1 km resolution near the time of hurricane landfall, about 150 km east of the hurricane center. Convective updrafts are indicated by the heavy bold contours of vertical velocity.